Journal of Manufacturing Systems
Vol. 22/No. 3
2002

Yield Improvement in Wafer Planarization: Modeling and Simulation

Sutee Eamkajornsiri, Dept. of Industrial and Manufacturing Systems Engineering, and **Ranga Narayanaswami** and **Abhijit Chandra,** Dept. of Mechanical Engineering, Iowa State University, Ames, Iowa, USA

Abstract

Chemical mechanical polishing (CMP) is a planarization process that produces high-quality surfaces both locally and globally. CMP is one of the key process steps during the fabrication of very large scale integrated (VLSI) chips in integrated circuit manufacturing. CMP consists of a chemical process and a mechanical process being performed together to reduce height variation across a wafer. High and reliable wafer yield, which is dependent on uniformity of the material removal rate across the entire wafer, is of critical importance in the CMP process. In this paper, the variations in the material removal rate across the wafer are analytically modeled assuming a rigid wafer and a flexible polishing pad. The wafer pad contact is modeled as the indentation of a rigid indenter on an elastic half-space. The model predictions are first verified against experimental observations. Simulation results for wafer yield under open-loop processing conditions are presented. Wafer curvature is identified as a key design variable influencing the spatial distribution of the material removal rate. The proposed model can be applied to control wafer-scale material removal rate variations in a CMP process.

Keywords: *CMP, Yield Improvement, Wafer Machining, Contact Mechanics, Nano-Scale Surfaces*

Introduction

Planarization technology is one of the key process steps during the fabrication of ultra large scale integrated/very large scale integrated (ULSI/VLSI) chips in integrated circuit (IC) manufacturing. The *chemical mechanical polishing* (CMP) process has emerged to be the most promising because of its demonstrated capability to provide better local and global planarization of wafer surfaces (Steigerwald, Murarka, Gutmann 1997).

In recent years, CMP has established itself as an enabling technology for the next generation of chip wiring and has become the second-fastest growing area of semiconductor equipment manufacturing (Stix 1998). Besides interlayer dielectric planarization, CMP has also found applications in shallow-trench isolation, damascene technologies (e.g., Kaanta et al. 1991; Kranenberg and Woerlee 1998), and other novel processing techniques such as polishing of Si_3N_4 balls for bearing applications (Jiang, Wood, Komanduri 1998).

CMP consists of a chemical process and a mechanical process being performed together to reduce height variation across a dielectric region. The chemical effects are the chemical reactions between the slurry and the wafer surface, which change the solubility and mechanical properties of the wafer surface, while mechanical processes are affected by the interface pressure, the rotational speed of the pad and the wafer, and the viscosity of the slurry (Chen and Lee 1999). The Preston equation (Preston 1927) summarizes the material removal rate (MRR) as follows:

$$\frac{dH}{dt} = K_P PV \tag{1}$$

where dH/dt is the MRR per unit surface area, P is the interface pressure, V is the relative velocity between the wafer and the polishing pad, and K_p is the Preston coefficient.

In the last several years, various researchers have attempted to modify the Preston equation to correct observed discrepancies with experimental observations. Zhang et al. (1999) proposed an equation, $MRR = K_p\sqrt{PV}$, taking into account the normal and shear stress acting on the contact area between abrasive particles and wafer surfaces. Zhao and Shi (1999) present $MRR = K_pP^{2/3}V$. They argue that the number of abrasives involved in material removal will increase with the contact area between the wafer and the pad, and because the MRR is linearly related to the number of abrasives, the MRR will be nonlinearly dependent on the pressure. Zhao and Shi also introduce the concept of a threshold pressure, arguing that material removal takes place only when the threshold pressure is exceeded. Luo and Dornfeld (2001) also introduce a nonlinear MRR model based on statistical distributions of abrasive particles. Fu et al. (2001) introduce another nonlinear MRR model based on the concept of incomplete and complete contact between the wafer and the pad. They also observe that the deviations of actual MRR predictions for these nonlinear models (particularly considering the level of confidence in these models) from Preston equation predictions can be small. This is particularly true when the slurry in a CMP process contains both sharp and blunt (spherical) abrasive particles. In view of this and the desire to keep the particle-scale MRR model simple, the Preston equation is adopted in the present work.

A schematic diagram of the CMP process is shown in *Figure 1*. In general, a CMP machine uses orbital, circular, and lapping motions. The wafer is held on a rotating carrier or wafer carrier, while the face being polished is pressed against a polishing pad attached to a rotating platen disk. Then the slurry that flows between the wafer and the pad is used as the chemical abrasive. CMP can be carried out on metals as well as on oxides.

Good wafer planarity, both local and global, is essential for the dimensional accuracy required at subsequent lithography stages of wafer manufacture. On a global scale, the within-wafer non-uniformity (WIWNU) is required to be within 0.2 μm across a 200 mm wafer. Even tighter tolerances become necessary as the wafer size increases and line width decreases (Byrne, Mullany, Young 1999).

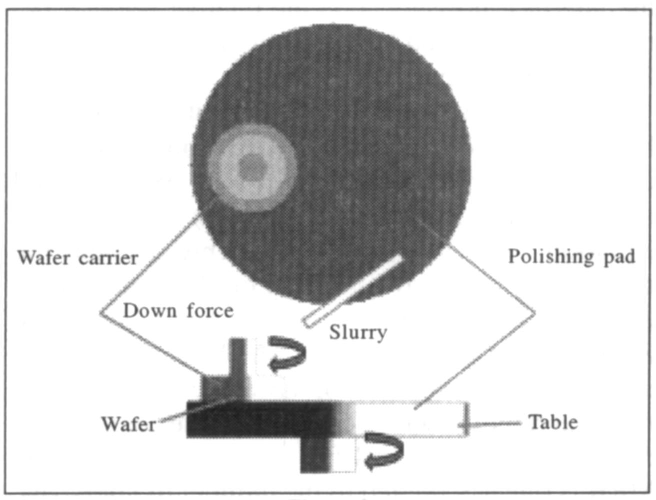

Figure 1
Illustration of CMP Process

There are two main concerns when considering global planarity of wafers:

(1) the edge-ring effect, where sharp variation in removal rate is observed near the edge of the wafer, and
(2) the less-severe variation in removal rate from the center to the periphery of the wafer.

For a typical 300 mm (dia) wafer, a 3 mm wide annular ring along the wafer periphery encompasses about 30% of the chips, which represents an annual revenue stream of about $2.7 billion per year for a single IC fabrication facility. Thus the issue of wafer-scale uniformity of the MRR has a significant impact on the yield from a wafer and is of critical importance to the IC manufacturing community.

Introducing the mechanics of beam bending, Sivaram et al. (1992) investigated wafer-scale variations in MRR by modifying Preston's equation via varying the contact pressure according to the deflection profile. They assume, however, that the section modulus (E*I) for the polishing pad is the same or higher than that of the platen, which is usually not the case. Runnels and Renteln (1993) focused on finite element modeling of the pad deflection and investigated wafer edge effects and wafer curvature effects during polishing. They observed that the normal pressure was uniform under the wafer except within one millimeter from the wafer edge. This does not explain the experimental observations, where a significant increase in MRR is observed over several millimeters (around 5 mm) from the edge of the wafer.

In the present work, the lower pad stiffness (compared to platen) is accommodated by treating the wafer pad contact as the indentation of a rigid indenter on an elastic half-space (Eamkajornsiri et al. 2001). The spatial variation of the interface pressure profile is incorporated into the Preston equation to obtain the spatial distribution of the MRR. This model accurately reflects the observed experimental variations in MRR over several millimeters from the wafer edge.

The wafer-scale model is used as a basis for simulating and controlling material removal in the CMP process. A subsequent paper will address the issues of controlling the process. The wafer-scale model allows the investigation of CMP process parameters such as down load, polishing time, pad properties, preexisting wafer curvature, and so on, on the yield. Therefore, model-based planning and control of the CMP process is possible and can serve as an alternative to the trial-and-error design procedure practiced today.

Wafer-Scale Modeling

Motivated by the observations that the WIWNU in the MRR is primarily caused by variations in contact pressure near the edge of a wafer, first an analytical expression is developed for the contact pressure distribution at the pad-wafer interface. It is assumed that material removal occurs primarily due to solid-solid contact, while the hydrodynamic effect is responsible for the slurry distribution.

Preexisting wafer curvature is modeled as a quadratic function $a_2 r^2$. As shown in *Figure 2*, the wafer is subjected to a rigid body displacement of a_0 due to the down load. The displacement field right under the wafer can therefore be expressed as follows:

$$f(r) = a_0 + a_2 r^2 \tag{2}$$

where r measures the radial distance from the center of the wafer, a_0 is the vertical displacement of the wafer (depth of penetration), and $2a_2$ is the wafer curvature caused by preexisting wafer bow. Given a fixed down load, the vertical displacement a_0 may be calculated from elastic indentation analysis. Using the simplest assumption of the pad as an elastic foundation, the down load $F = ka_0$ when k is the spring constant for the pad. Typical down pressures used in CMP are in the range 1 to 10 psi. The parameter a_0 scales with the magnitude of the down load on the wafer.

Considering the friction in the hoop direction only, and neglecting the friction in the radial direction, the overall contact problem may be formulated (see *Figure 2*) with the following boundary conditions at $z = 0$ (the free surface of the pad):

$$\tau_{zr} = 0 \ (0 \leq r < \infty)$$

$$\sigma_{zz} = 0 \ (r > a)$$

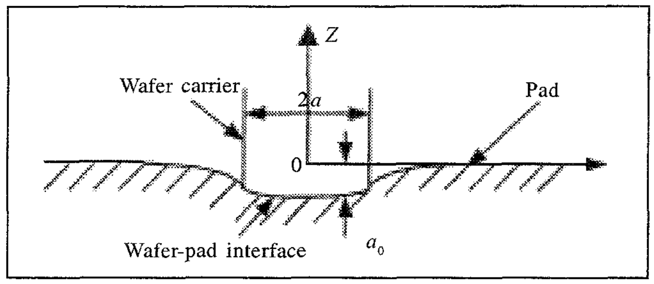

Figure 2
Model of Pad and Wafer Contact. a_0 is a rigid body displacement of wafer due to down load and $2a$ is the wafer diameter

$$\tau_{z\theta} = 0 \ (r > a)$$

$$u_z = f(r) \text{ and } \tau_{z\theta} = \mu\sigma_{zz} \ (0 \leq r < a)$$

where $f(r)$ describes the position of the wafer, τ_{zr} and $\tau_{z\theta}$ are the shear stresses, σ_{zz} is the normal stress (contact pressure), and μ is the friction coefficient.

This problem can be decomposed into two cases with a weak coupling between them (Gladwell 1980; Johnson 1985; Fu and Chandra 2001, 2002) and solved by superposition. The cases are given as follows.

Case I

The boundary conditions at $z = 0$ are as follows:

$$\tau_{zr}^{(I)} = 0, (0 \leq r < \infty)$$
$$\tau_{z\theta}^{(I)} = 0, (0 \leq r < \infty)$$
$$\sigma_{zz}^{(I)} = 0, (r > a)$$
$$u_z^{(I)} = f(r), (0 \leq r \leq a)$$

Case II

The boundary conditions at $z = 0$ are as follows:

$$\tau_{zr}^{(II)} = 0, (0 \leq r < \infty)$$
$$\sigma_{zz}^{(II)} = 0, (0 \leq r < \infty)$$
$$\sigma_{z\theta}^{(II)} = 0, (r > a)$$
$$\tau_{z\theta}^{(II)} = \mu\sigma_{zz}^{(I)}, (0 \leq r \leq a)$$

By superposition of case I and case II, the final solution to the original problem can be obtained as follows (where k is the order of the polynomial, $k = 2$ for the present case; G is the hyperbolic function; and F_1 is the hypergeometric function):

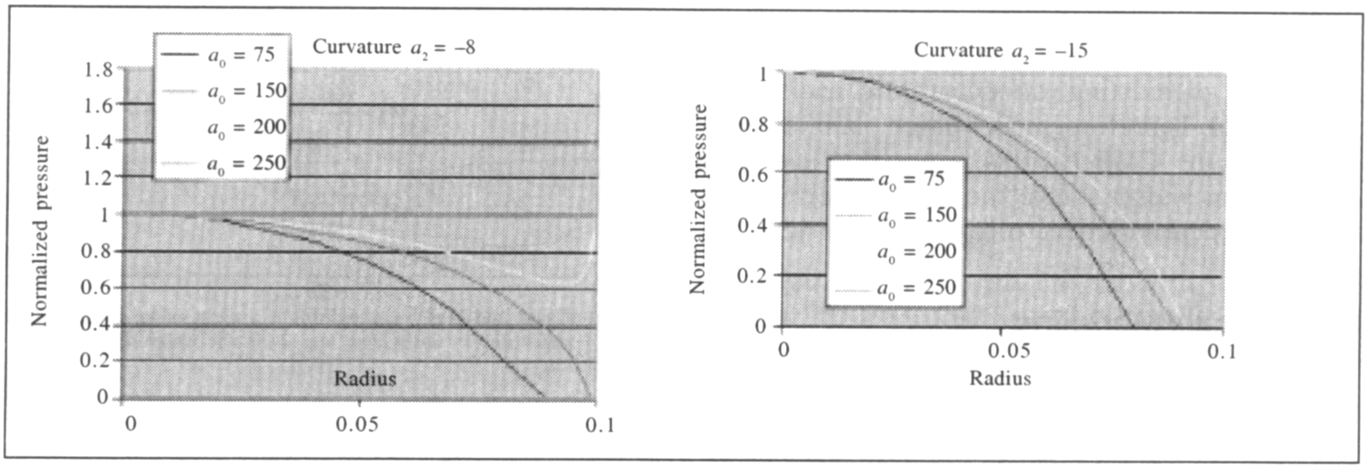

Figure 3
Normalized Pressure Profile Curves Shown for Two Values of Curvature a_2 ($\times$ 10^{-6} m^{-1}) and Several Values of Indentation Depth a_0 (nm). Wafer radius is 0.1 m.

$$\sigma_{zz}\big|_{z=0} = \sigma_{zz}^{(1)}\big|_{z=0} =$$

$$-\frac{1}{2\sqrt{\pi}}\cdot\frac{E}{1-\nu^2}\sum_{k=0}^{n} a_k (1+k)\cdot a^{1+k}\cdot\frac{\Gamma\left(\frac{2+k}{2}\right)}{\Gamma\left(\frac{3+k}{2}\right)}\cdot\left\{\frac{1}{r^2}\left[\frac{1}{\sqrt{1-\frac{r^2}{a^2}}}\,{}_2F_1\left(\frac{1}{2};-\frac{1+k}{2};\frac{1-k}{2};\frac{r^2}{a^2}\right)\right]\right\}$$

The pressure distribution on the contact area (Fu and Chandra 2001, 2002) can be expressed as follows (with $k = 2$):

$$P(r) = K\frac{4a_2r^2 + \left(a_0 - 2a_2a^2\right)}{\left(a_0 - 2a_2a^2\right)\sqrt{1-\left(\frac{r}{a}\right)^2}} \tag{3}$$

where r is any arbitrary radius, a is the radius of the wafer, and K is a constant that depends on the pad properties. This constant is different from K_p, the Preston coefficient mentioned in Eq. (1).

The normalized pressure is the pressure at any radius divided by the pressure at the center of the wafer. The normalized pressure may be obtained by setting $K = 1$ in Eq. (3). *Figure 3* is a plot of the normalized pressure profiles for a variety of load (a_0) and two curvature (a_2) values. In *Figure 3a*, the curvature is set to -8×10^{-6} m^{-1} and the load is varied corresponding to indentation depth (a_0) variation from 25 nm to 250 nm. For low load, the pressure profiles slope downward, and as the load increases, the pressure at the edge starts rising. At high loads, the increase in pressure at the edge is even higher. For a curvature of -15×10^{-6} m^{-1}, the pressure profiles are downward sloping, as shown in *Figure 3b*. In Eq. (3), if the pressure turns out to be negative, it is set to zero. This corresponds to loss of contact between the pad and the wafer. In CMP, the pressure profile controls the material removal rate. A uniform pressure profile would result in the best surface. It is to be noted that the curvature is continuously changing as material is removed. The pressure profiles should be chosen such that they are uniform or they are compensating in the sense that upward-sloping pressure profiles are matched up with downward-sloping pressure profiles to result in a good wafer surface.

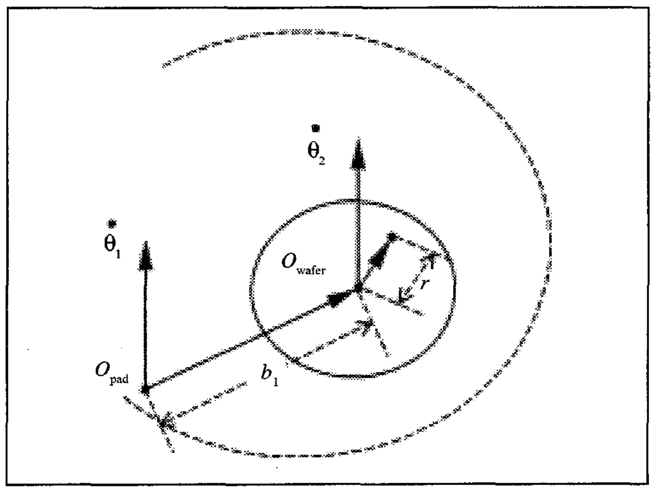

Figure 4
Kinematics of CMP Process

Based on the kinematics as depicted in *Figure 4*, the magnitude of the polishing velocity, which is the relative velocity between the pad and the wafer (Chen and Lee 1999), can be written as follows:

$$\left|V_p\right| = \left|\dot{\theta}_1\right| \left(b_1^2 + r^2 (k_v - 1)^2 - 2 b_1 r (k_v - 1) \cos\theta_2 \right)^{1/2} \quad (4)$$

where $\dot{\theta}_1$ is the angular velocity of the polishing pad, b_1 is the offset distance between the axes of the pad and the wafer, r is an arbitrary radius on the wafer, and k_v is the ratio of the angular velocity of the wafer to the angular velocity of the pad. θ_2 can be expressed as follows:

$$\theta_2 = \left(\dot{\theta}_2 - \dot{\theta}_1\right)t \quad (5)$$

where $\dot{\theta}_2$ is the angular velocity of the wafer and t is the processing time.

The MRR per unit area may now be calculated at any point in space and time by substituting the instantaneous values of pressure and velocity at a particular location in Eq. (1). The height removed may be obtained by integrating dH/dt over time.

Comparison to Experimental Observations

To compare model predictions against experimental observations, it is first assumed that the MRR follows Preston's equation. Thus, MRR (and the residual film thickness) at a spatial location is assumed to vary linearly with the contact pressure at that location.

Model predictions for a wafer profile described as a parabola ($a_2 = 5 \times 10^{-6}$ inch^{-1}) with indentation depth ($a_0 = -2.0 \times 10^{-4}$ inch) are compared to the experimental observations of WIWNU in the MRR by Srinivasa Murthy et al. (1997). Their experiments were carried out with an R200T3 carrier film with modulus of elasticity of 10 psi. A down pressure of 7 psi, platen speed of 28 rpm, and carrier speed of 32 rpm were used. The slurry used was SS12 and the pad was IC1000/SUBA IV (both from Rodel Inc.). The wafer was 8 inches in diameter (a = 4 inches). *Figure 5* shows a comparison of the model prediction with the experimental MRR distribution. The model predicts an almost constant MRR in the center region and a very high MRR at the wafer edge, which are consistent with the experimental observations. It may be observed that the model predictions compare well with the experimental data so long as the radial distance does not exceed 3 inch (for a 4 inch radius wafer). The model also captures the extreme variation at the wafer edge. However, within an annular region of 1 inch from the wafer edge, the rigid wafer model does not capture the local peak-and-valley type of variation in the MRR. Recently, it has been observed that a flexible wafer model (Fu 2002) is capable of capturing such variation.

Wafer Yield Simulation

The wafer yield is the number of good dies at the end of a CMP process cycle. A wafer is divided into rectangular sectors called dies. After CMP processing is complete, the dies are sawed off and used in subsequent IC fabrication. A die is classified as good if at CMP stopping time all the four corners of the die are within tolerance. For productivity, it is critical to have a high wafer yield, and thus, effective choice of the CMP process parameters is important.

A magnified view of the oxide layer on the wafer surface, with the preexisting curvature a_2 and the indentation depth a_0, is shown in *Figure 6*. Considering the Z axis to be pointing downward from the base of the oxide surface, the profile of the oxide layer as a function of space and time can be represented as follows:

$$z(0, r) = O_{\text{nom}} + a_2(0)r_2$$

$$z(t + \Delta t, r) = z(t, r) - K_p P(r) V \Delta t \quad (6)$$

where O_{nom} is the thickness of the oxide layer at the center of the wafer. At the beginning of CMP, the wafer curvature is the preexisting wafer curvature and is denoted as $a_2(0)$. As the polishing progresses, the curvature at each step, $a_2(t)$, is recomputed by a least-squares fit of the updated wafer profile. The interface pressure profile can now be computed using Eq. (3). The wafer profile can thus be traced out with time. The goal of CMP is to generate a flat surface on the oxide layer. The CMP process should be stopped when the yield is at a maximum. Stopping criteria are thus very important.

As an example, the wafer yield for the CMP process parameters as selected below is simulated.

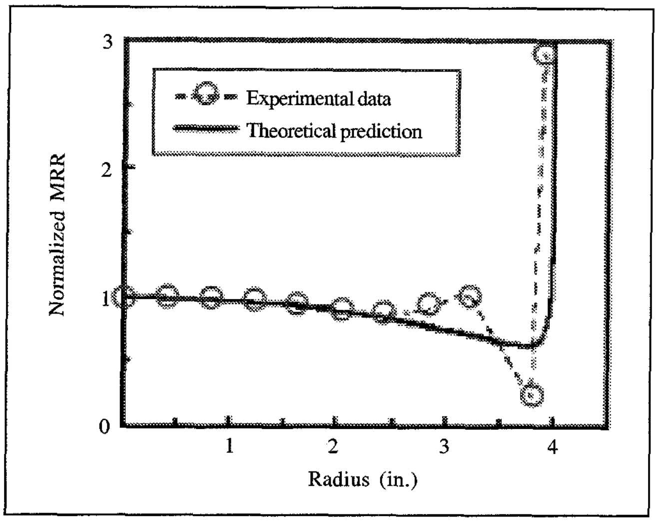

Figure 5
Comparison of Model-Predicted MRR Against Experimental Observations of Srinivasa Murthy et al. (1997)

- Down pressure is 6 psi
- Pad angular velocity is 35 rpm
- Wafer angular velocity is 20 rpm
- Wafer diameter is 200 mm
- Offset distance between the axes of the pad and the wafer is 170 mm
- $K_p = 11.2 * 10^{-10}$ 1/psi
- Oxide thickness is 8000 Å (angstroms)
- Desired final surface height is 1000 Å (after finishing CMP)
- Tolerance is 200 Å

At the down load of 6 psi, the a_0 value is 200 nm. If the initial wafer curvature, a_2, is taken as -10×10^{-6} m^{-1}, the best yield is 200 out of a best possible 268 and occurs at time 104 sec. A progression of the wafer yield is shown in *Figure 7*. Initially, all the dies are underpolished (94 sec. and 98 sec.). As CMP time progresses, the dies at the edge of the wafer come into tolerance and quickly get overpolished; however, the dies at the interior of the wafer are still underpolished (102 sec.). As CMP time still progresses, the dies in the interior of the wafer come into tolerance; however, dies at the edge of the wafer are now overpolished (106 sec.). The actual curvature of the wafer is progressively reduced as CMP progresses. As the curvature reduces, the pressure profile curves change from downward-sloping curves to upward-sloping curves. This causes a higher polishing rate at the edge of the wafer. Consequently, the edge of the wafer tends to be overpolished first. The wafer yield for three starting values of curvature, a_2, is shown in *Figure 8*. From this figure, it is clear that the wafer yield is high momentarily and diminishes very quickly. The curvature variation with CMP time is shown in *Figure 9*, and the pressure profile variation when a_2 is -10×10^{-6} m^{-1} is shown in *Figure 10*. Based on the observations of Ouma (1998), the velocity, V, in these simulations is taken to be the value at the edge of the wafer for the purpose of simplicity.

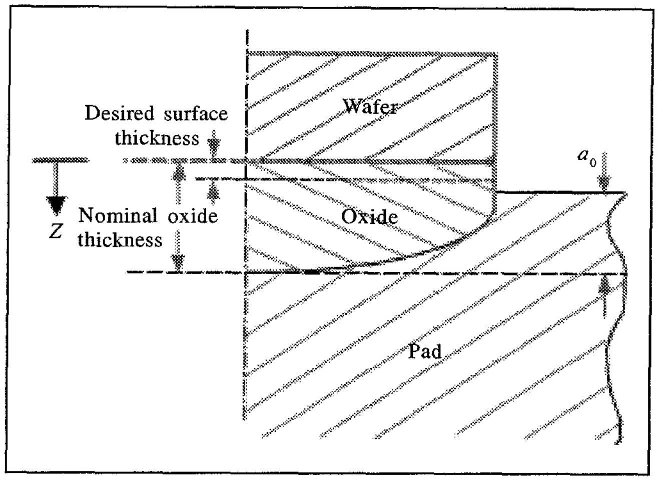

Figure 6
Detailed View of Oxide Layer on Wafer Polished in CMP

Discussion and Conclusion

Within wafer non-uniformity (WIWNU) in material removal rate (MRR) is a critical parameter in determining the quality of a wafer planarized by a CMP process. This paper presents a model-based simulation for predicting the WIWNU in the MRR and the associated wafer yield for a CMP process. A solid-solid contact model is assumed for material removal. The pad is modeled as an elastic half-space, indented by a rigid wafer.

The model-based graphical simulations confirm that the edge effect is mainly caused by the configuration of the CMP setup and process parameters. The temporal and spatial variation of pressure distribution based on the wafer-scale model can thus be very useful in predicting wafer yield and determining the stopping time. More importantly, the model can serve as a method for planning and controlling the CMP process.

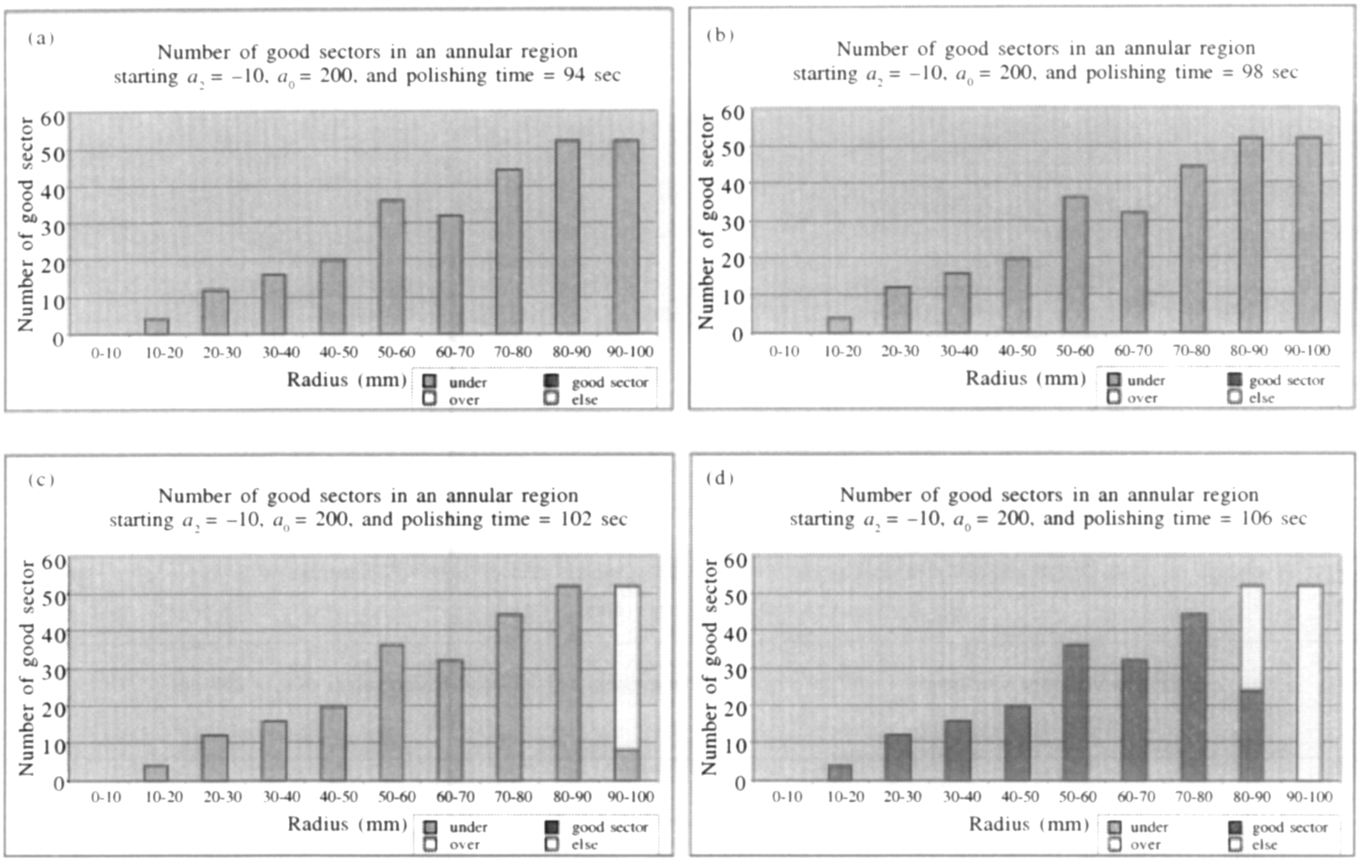

Figure 7

Progression of Wafer Yield in an Open-Loop CMP Process. Wafer curvature is –10 × 10^{-6} m^{-1} and applied load is equivalent to a_0 = 200 nm. (a) At polishing time = 94 sec., (b) At polishing time = 98 sec., (c) At polishing time = 102 sec., (d) At polishing time = 106 sec. Overpolishing occurs at the periphery and diminishes yield. Best yield is 200 at 104 sec.

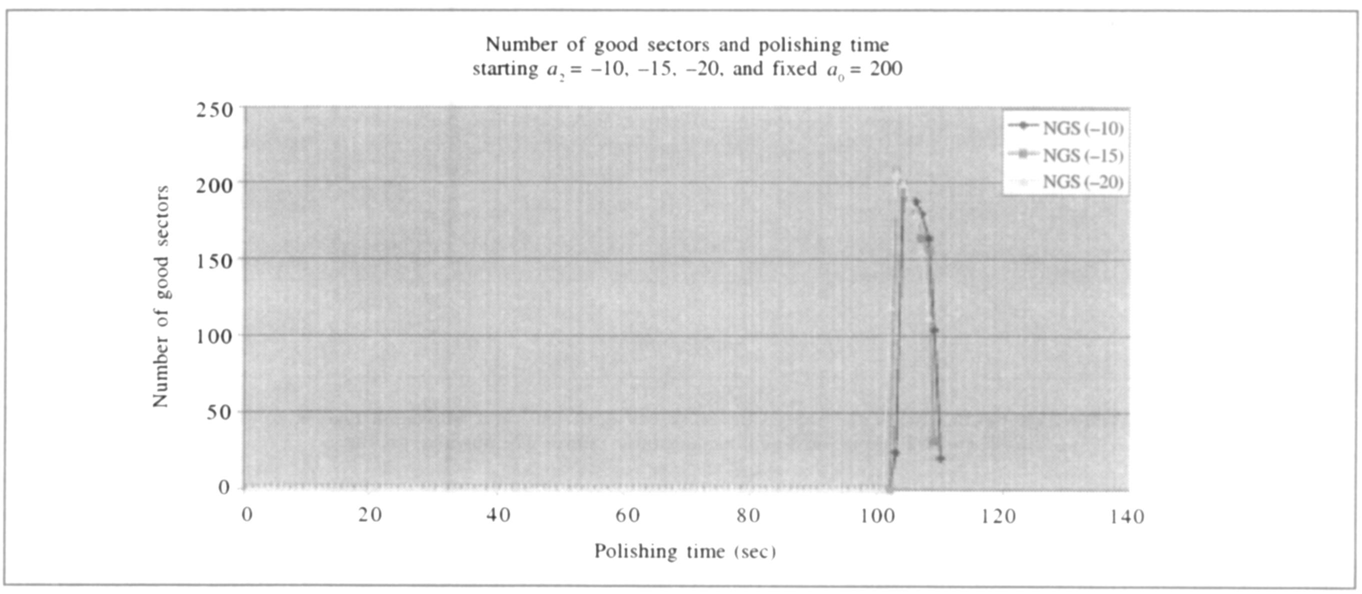

Figure 8

Wafer Yield with Polishing Time. Wafer curvatures are –10 × 10^{-6} m^{-1}, –15 × 10^{-6} m^{-1}, –20 × 10^{-6} m^{-1}, and applied load is equivalent to a_0 = 200 nm. Wafer yield is high only for a very short time period, making CMP stopping time estimation a very important parameter.

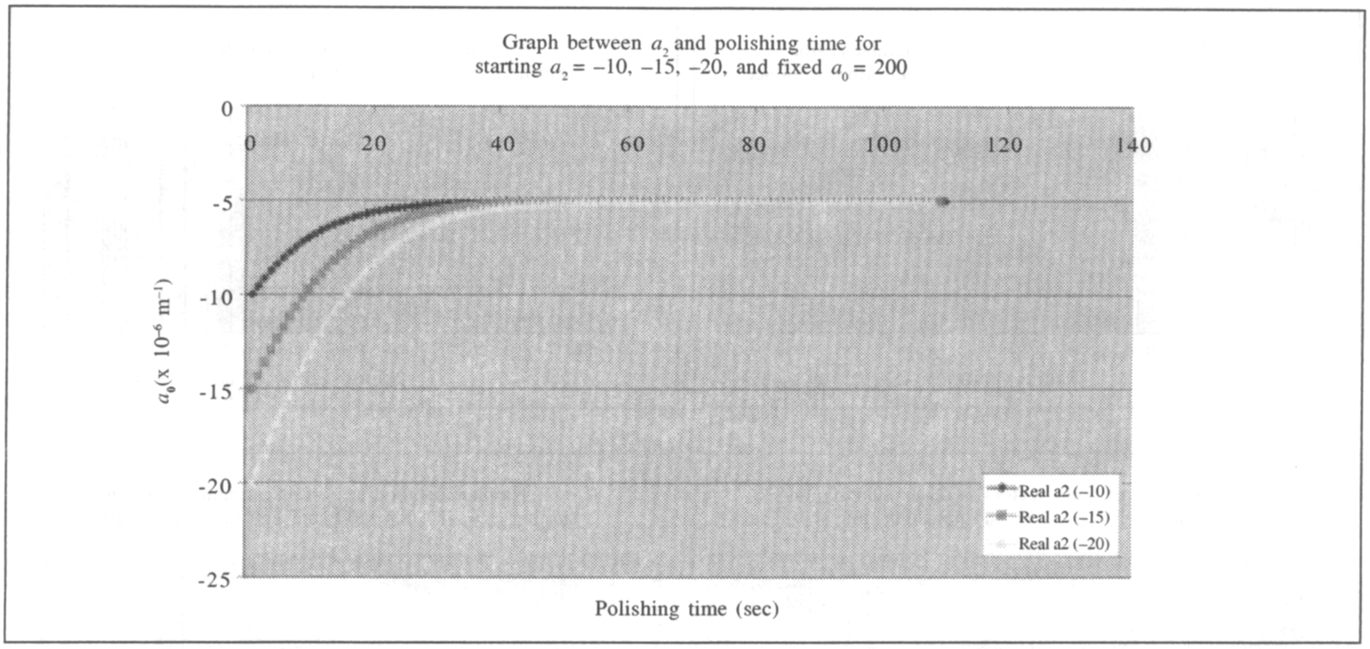

Figure 9
Variation of Wafer Curvature (× 10^{-6} m^{-1}) as CMP Progresses. Applied load is equivalent to a_0 = 200 nm.

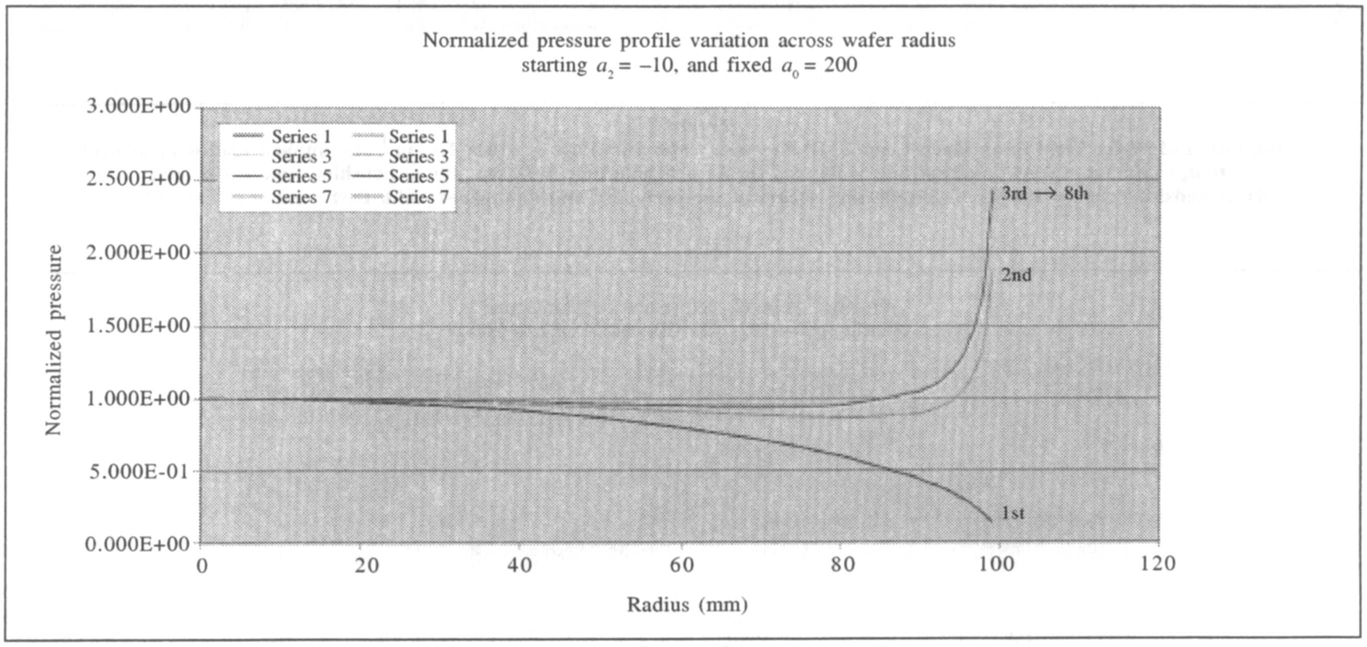

Figure 10
Pressure Profile Patterns in CMP with Wafer Curvature −10 × 10^{-6} m^{-1} and equivalent load of a_0 = 200 nm. Initial curve is downward sloping and later curves are upward sloping.

Current CMP industry practice uses mostly open-loop load control. The present model identifies the wafer curvature as a critical parameter as well, affecting the interface pressure profile. By varying the curvature, the spatial pressure distribution can be modified from a downward-sloping (edge slow) to an upward-sloping (edge fast) profile. This can be utilized for effectively controlling the polishing process so that the total material removed over the entire wafer is uniform at the stopping time. The model-based simulation is also capable of identifying the optimum polishing time for maximization of wafer yield. A control strategy based on the above modeling capability is being actively developed and validated and will be presented in a future paper.

Acknowledgment

The authors gratefully acknowledge the financial support provided under NSF grant no. DMI 0084736 and DMI 0323069. Any opinions, findings, and conclusions or recommendations expressed in this material are those of the authors and do not necessarily reflect the views of the National Science Foundation.

References

Byrne, G.; Mullany, B.; and Young, P. (1999). "The effect of pad wear on the chemical mechanical polishing of silicon wafers." *Annals of the CIRP* (v48, n1), pp143-146.

Chen, D.Z. and Lee, B.S. (1999). "Pattern planarization model for chemical mechanical polishing." *Journal of the Electrochemical Society* (v146, n2), pp744-748.

Eamkajornsiri, S.; Fu, G.; Narayanaswami, R.; and Chandra, A. (2001). "Simulation of wafer scale variations in chemical mechanical polishing." *Trans. of NAMRI/SME* (v29). Dearborn, MI: Society of Manufacturing Engineers, pp221-228.

Eamkajornsiri, S.; Narayanaswami, R.; and Chandra, A. (2002). "Wafer yield improvement in CMP: load and curvature control." In review for the *Journal of Manufacturing Systems*.

Fu, G. (2002). "Modeling of chemical mechanical polishing at multiple scales." PhD thesis. Ames, IA: Dept. of Mechanical Engg., Iowa State Univ.

Fu, G. and Chandra, A. (2001). "A model for wafer scale variation of removal rate in chemical mechanical polishing based on elastic pad deformation." *Journal of Electronic Materials* (v30), pp400-408.

Fu, G. and Chandra, A. (2002). "Normal indentation of elastic half-space with a rigid frictionless axisymmetric punch." *ASME Journal of Applied Mechanics* (in press).

Fu, G.; Chandra, A.; Guha, S.; and Subhash, G. (2001). "A plasticity based model of material removal in chemical mechanical polishing (CMP)." *IEEE Trans. on Semiconductor Mfg.* (v14, n4), pp406-417.

Gladwell, G.M.L. (1980). *Contact Problems in the Classical Theory of Elasticity*. Alphen ann Rijin, Netherlands: Silthoff and Noordhoff Int. Publishers.

Jiang, M.; Wood, N.; and Komanduri, R. (1998). "On the chemo-mechanical polishing (CMP) of Si_3N_4 bearing balls with water based CeO_2 slurry." *ASME Journal of Engg. Materials Technology* (v120), pp304-312.

Johnson, K.L. (1985). *Contact Mechanics*. Cambridge, UK: Cambridge Univ. Press.

Kaanta, C.W.; Bombardier, S.G.; Cote, W.J.; Hill, W.R.; Kerzkowski, G.; Landis, H.S.; Poindexter, D.J.; Pollard, C.W.; Ross, G.H.; Ryan, J.G.; Wolff, S.; and Cronin, J.R. (1991). "Dual damascene: a ULSI wiring technology." *Proc.* of VMIC Conf., pp144-152.

Kranenberg, H. and Woerlee, P.H. (1998). "Influence of overpolish time on the performance of W damascene technology." *Journal of the Electrochemical Society* (v145, n4), pp1285-1291.

Luo, J. and Dornfeld, D.A. (2001). "Material removal mechanism in chemical mechanical polishing: theory and modeling." *IEEE Trans. on Semiconductor Mfg.* (v14, n2), pp112-132.

Ouma, D.O. (1998). "Modeling of chemical mechanical polishing for dielectric planarization." PhD thesis. Cambridge, MA: Dept. of Electrical Engg. and Computer Science, Massachusetts Institute of Technology.

Preston, F.W. (1927). "The theory and design of plate glass polishing machine." *Journal of the Society of Glass Technology* (v11, n44), pp214-256.

Runnels, S.R. and Renteln, P. (1993). "Modeling the effects of polish pad deformation on wafer surface stress distributions during chemical-mechanical polishing." *Dielectric Science and Technology*, pp110-121.

Sivaram, S.; Bath, H.; Lee, E.; Leggett, R.; and Tolles, R. (1992). "Measurement and modeling of pattern sensitivity during chemical mechanical polishing of interlevel dielectrics." SEMATECH Technical Report, Austin, TX.

Srinivasa Murthy, C.; Wang, D.; Beaudoin, S.P.; Bibby, T.; Holland, K.; and Cale, T.S. (1997). "Stress distribution in chemical mechanical polishing." *Thin Solid Films* (v308-309), pp533-537.

Steigerwald, J.M.; Murarka, S.P.; and Gutmann, R.J. (1997). *Chemical Mechanical Planarization of Microelectronic Materials*. New York: John Wiley & Sons.

Stix, G. (1998). "Faster smaller flatter." *Scientific American* (Feb. 1998), pp34-35.

Zhang, F.; Busnaina, A.A.; Feng, J.; and Fury, M.A. (1999). "Particle adhesion force in CMP and subsequent cleaning processes." *Proc.* of 4th Int'l Chemical-Mechanical Planarization for ULSI Multilevel Interconnection Conf., Santa Clara, CA, Feb. 1999, pp61-64.

Zhao, B. and Shi, F.G. (1999). "Chemical mechanical polishing in IC processes: new fundamental insights." *Proc.* of 4th Int'l Chemical-Mechanical Planarization for ULSI Multilevel Interconnection Conf., Santa Clara, CA, Feb. 1999, pp13-22.

Authors' Biographies

Sutee Eamkajornsiri is a doctoral candidate in the Dept. of Industrial and Manufacturing Systems Engineering at Iowa State University. His research interests are in developing yield improvement techniques for chemical mechanical polishing. E-mail: *suteejoe@iastate.edu*.

Ranga Narayanaswami is an assistant professor in the Dept. of Industrial and Manufacturing Systems Engineering at Iowa State University. His research interests are in computer-aided design, geometric modeling, multiresolution methods in CAD/CAM intelligent CAD systems, and modeling and optimization of manufacturing processes and systems. He holds a PhD in mechanical engineering from the University of California at Berkeley and a BS from the Indian Institute of Technology at Madras. E-mail: *ranga@iastate.edu*.

Abhijit Chandra is the Engel Professor of Mechanical Systems and Director of the Engel Manufacturing Lab in the Dept. of Mechanical Engineering at Iowa State University. He holds a PhD in mechanical engineering from Cornell University and a BS in mechanical engineering from the Indian Institute of Technology at Kharagpur. His research interests are in mechanics of manufacturing processes, nanoscale surface modification, and application of the boundary element method. E-mail: *achandra@iastate.edu*.